Di-hadron correlations with event shape engineering in Au+Au collisions at STAR

Ryo Aoyama, for the STAR Collaboration

University of Tsukuba, TCHoU

Oct. 25th, 2018

Joint Meeting of the APS DNP and JPS @Hawaii

STAR

U.S. DEPARTMENT OF ENERGY | Office of Science

筑波大学 University of Tsukuba

Tomonaga Center for the History of the Universe

Jets with di-hadron correlations in heavy-ion collisions

- ✦ Jets interact with colored matter and lose their energy : jet quenching
  - ‣ probe energy loss mechanisms in the QGP
- ✦ **high-p_T** : disappearance of back-to-back jet-like peak in central Au+Au collisions
  - ‣ jet suppression in the QGP

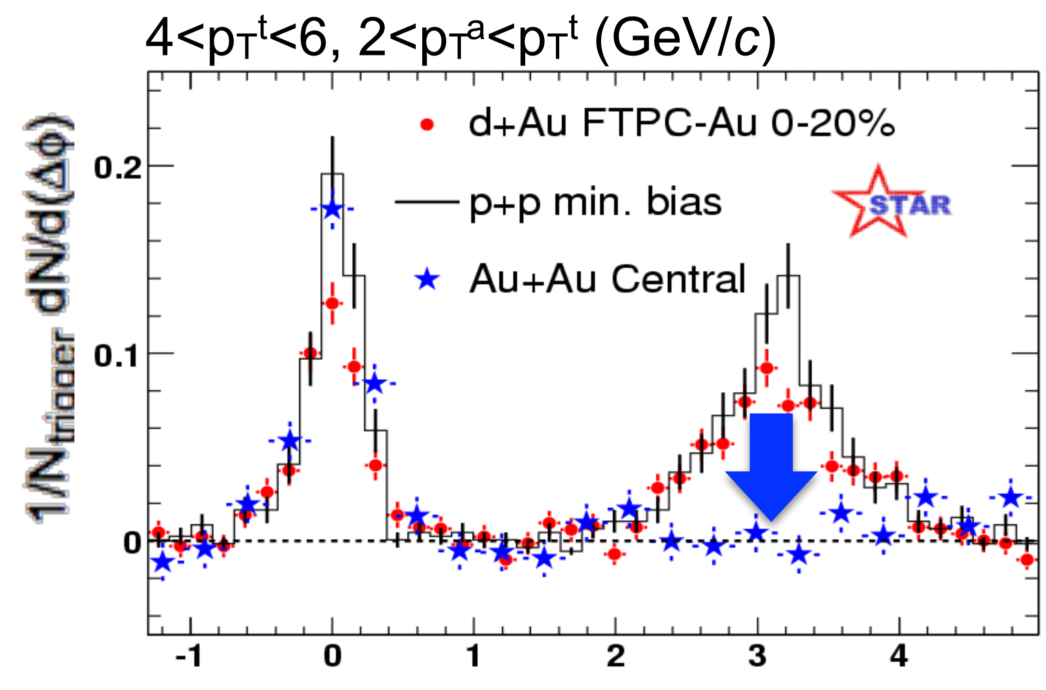

STAR, PRL 91, 072304 (2003)

only v_2 subtraction

- ✦ **low-p_T** : enhanced yield on both near and away side compared to p+p collisions
  - ‣ re-distribution of deposited energy

PHENIX, PRC 78, 014901 (2008)

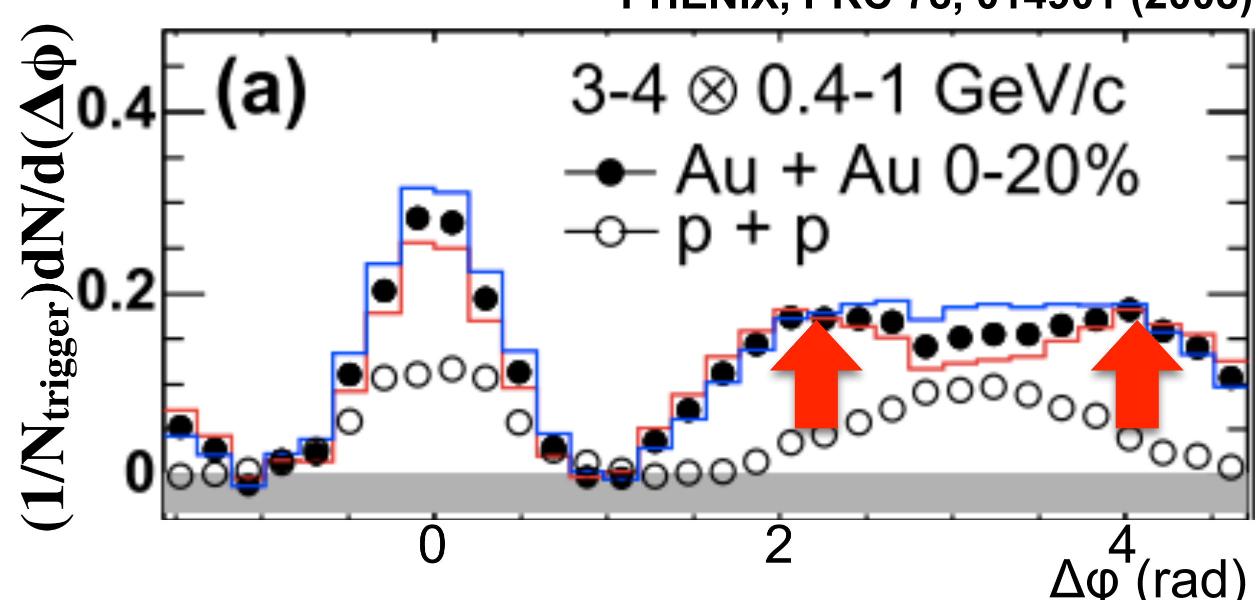

only v_2 subtraction

Event plane and higher order flow harmonics

✦ Spatial anisotropy due to **almond-like shape** and **event-by-event fluctuations** of overlapping region of nuclei in non-central heavy-ion collisions

✦ Deformation converted into momentum space by **collective motion** (**flow**)

- azimuthal anisotropy

azimuthal distribution : $\frac{dN}{d\phi} \propto 1 + \sum_i 2v_n \cos n(\phi - \Psi_n)$

n-th order event plane : $\Psi_n = \frac{1}{n} \cdot \frac{\sum w_i \sin(n\phi_i)}{\sum w_i \cos(n\phi_i)}$

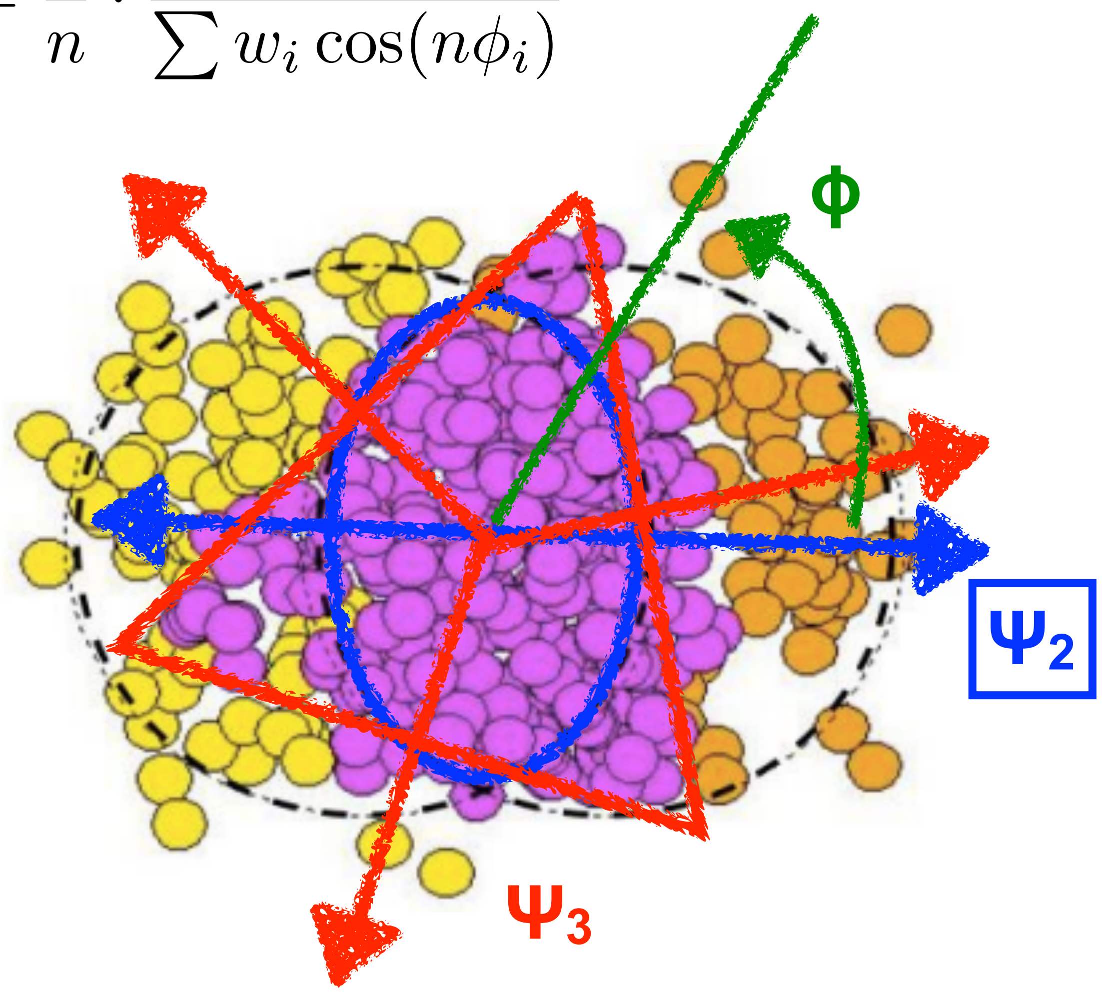

Event plane dependent di-hadron correlations

STAR, PRC 89, 041901 (2014)

ϕ_s : trigger angle with respect to event plane ($=\phi-\Psi_2$)

v_2, v_3, v_4 subtracted

in-plane ⟷ out-of-plane

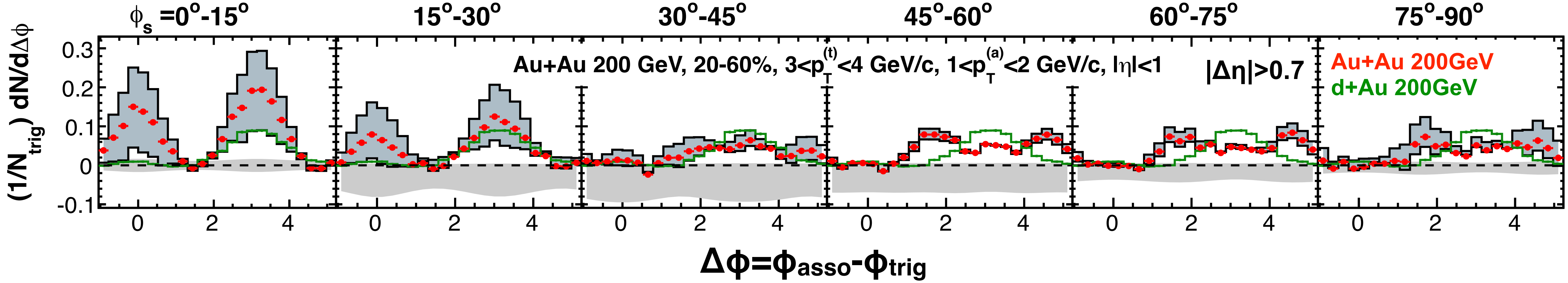

- ✦ Possibility of control in-medium path length of jets
- ✦ EP dependence of jet-medium interactions
  - Single peak by the in-plane trigger in the away side
  - Away-side peak becomes lower and broadened as trigger direction changes from in-plane to out-of-plane

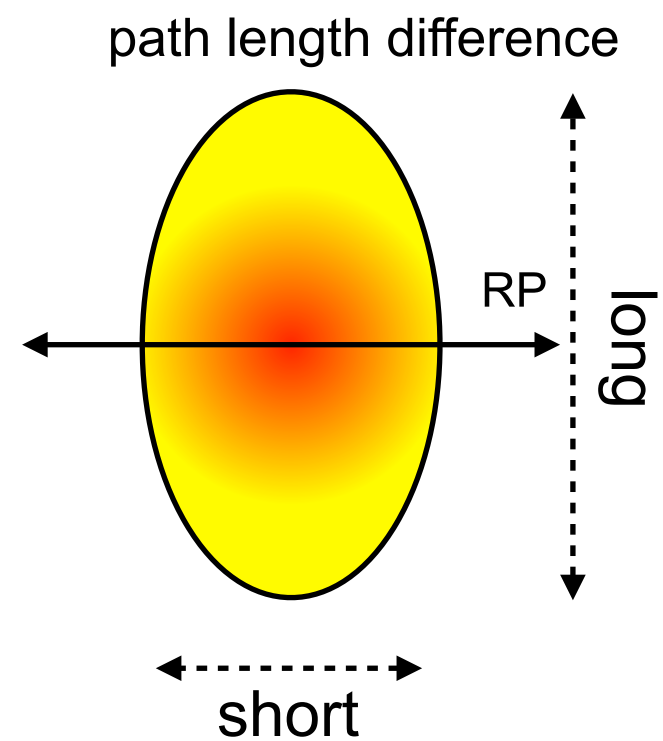

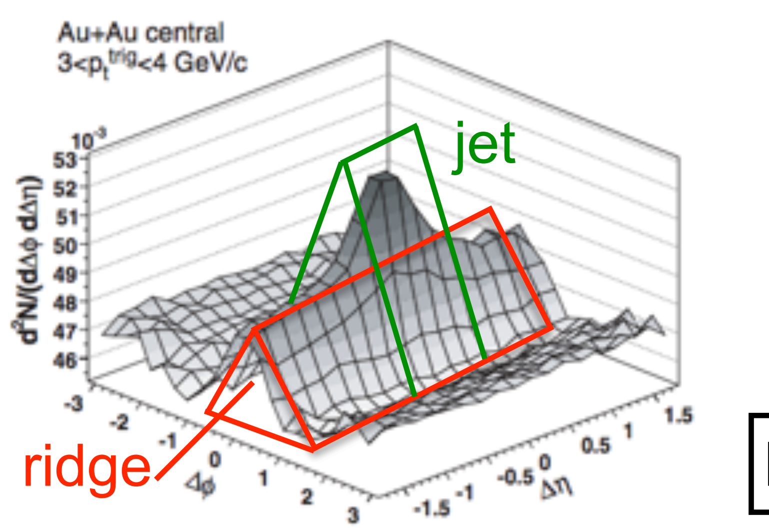

STAR, PRC 80, 064912 (2009)

Rest of this talk : **|Δη|<1** ▶ jet cone AND away-side are focused on

Event plane dependent di-hadron correlations

STAR, PRC 89, 041901 (2014)

v_2, v_3, v_4 subtracted

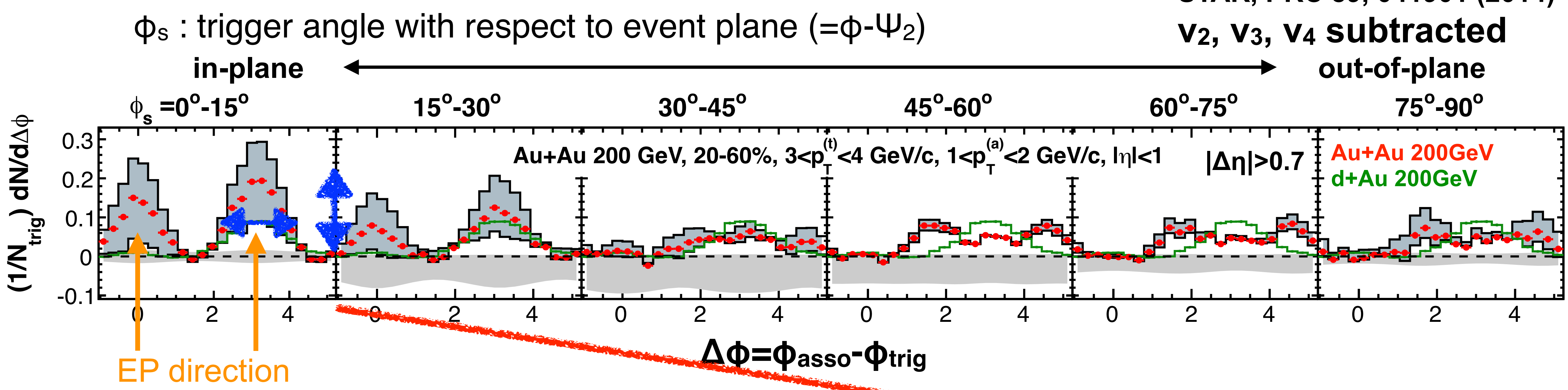

- ✦ Possibility of control in-medium path length of jets
- ✦ EP dependence of jet-medium interactions
  - Single peak by the in-plane trigger in the away side
  - Away-side peak becomes lower and broadened as trigger direction changes from in-plane to out-of-plane

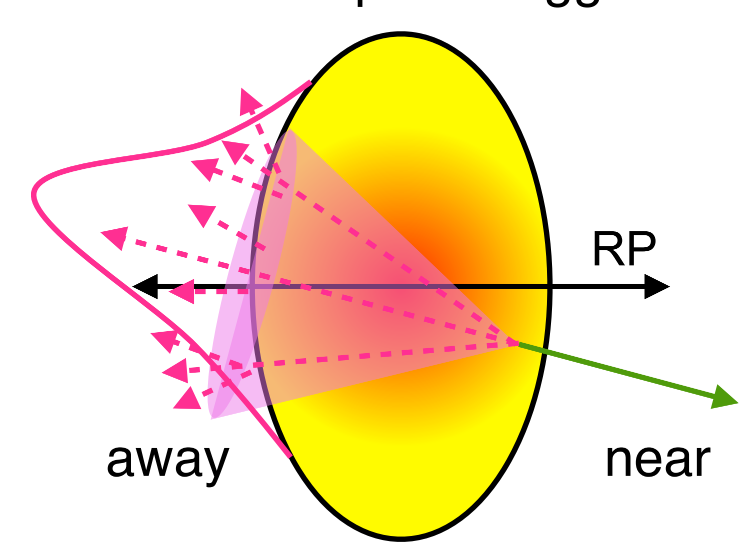

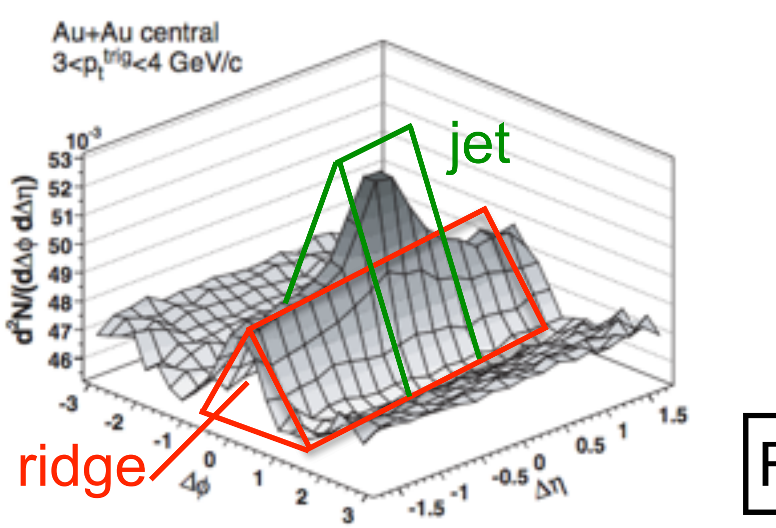

STAR, PRC 80, 064912 (2009)

Rest of this talk : **|Δη|<1** ▶ jet cone AND away-side are focused on

Event plane dependent di-hadron correlations

STAR, PRC 89, 041901 (2014)

ϕ_s : trigger angle with respect to event plane ($=\phi-\Psi_2$)

v_2, v_3, v_4 subtracted

in-plane ⟷ out-of-plane

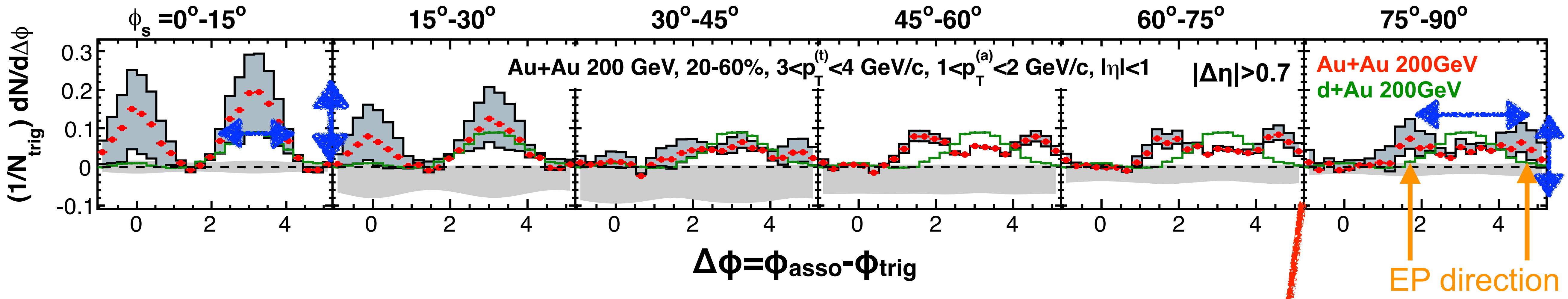

- ✦ Possibility of control in-medium path length of jets
- ✦ EP dependence of jet-medium interactions
  - Single peak by the in-plane trigger in the away side
  - Away-side peak becomes lower and broadened as trigger direction changes from in-plane to out-of-plane

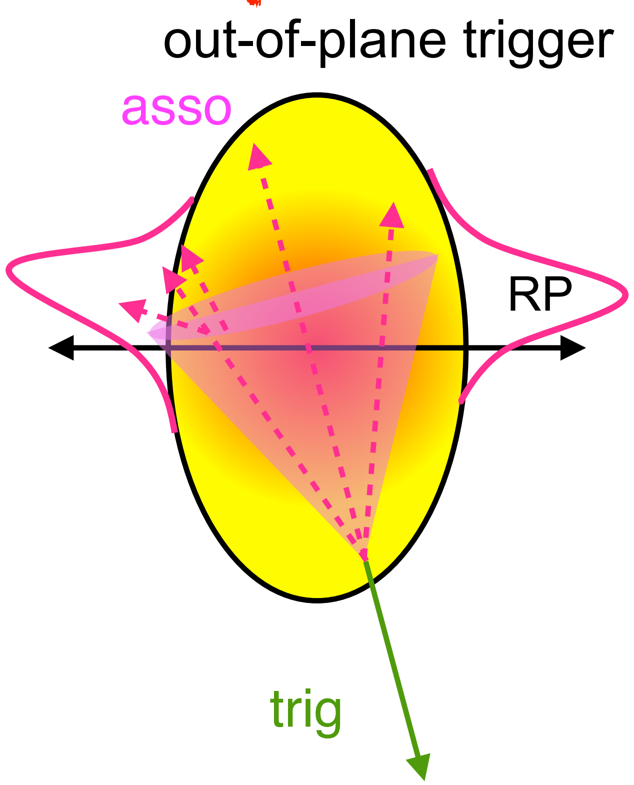

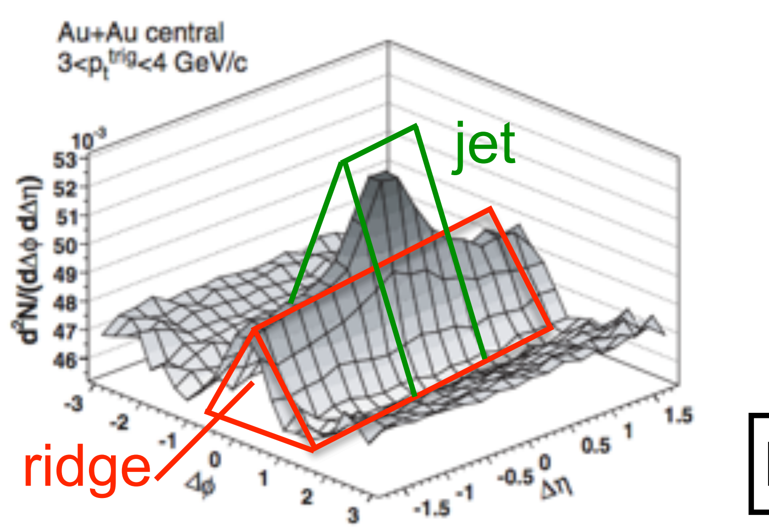

STAR, PRC 80, 064912 (2009)

Rest of this talk : **|Δη|<1** ▶ jet cone AND away-side are focused on

Event shape engineering (ESE)

- Selection of event-by-event flow amplitude
  - event-by-event v_2 largely fluctuates in a fixed centrality bin
  - control fluctuating v_2 by selecting the magnitude of flow vector q_2
  - Possibility to control the initial geometry

J.Schukraft, A.Timmins and S.A.Voloshin, PLB 719 (2013), 394-398

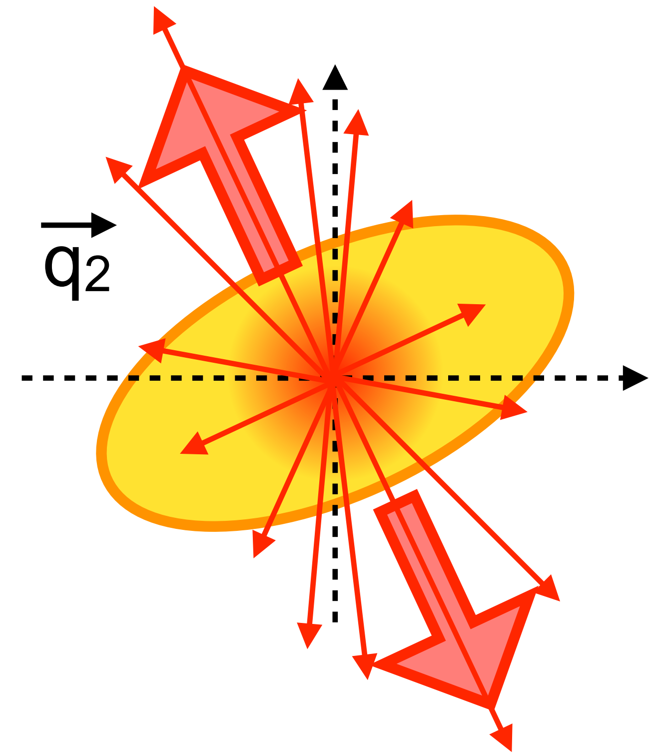

$$Q_{2,x} = \sum w_i \cos(2\phi_i) / \sqrt{\sum w_i}$$
$$Q_{2,y} = \sum w_i \sin(2\phi_i) / \sqrt{\sum w_i}$$
$$q_2 = \sqrt{Q_{2,x}^2 + Q_{2,y}^2}$$

w_i : weighting factor

A.M.Poskanzer, S.A.Voloshin, PRC 58 (1998), 1671-1678

initial eccentricity $\varepsilon_2 = \frac{\langle x^2 - y^2 \rangle}{\langle x^2 + y^2 \rangle}$

correlation between q_2 and ε_2

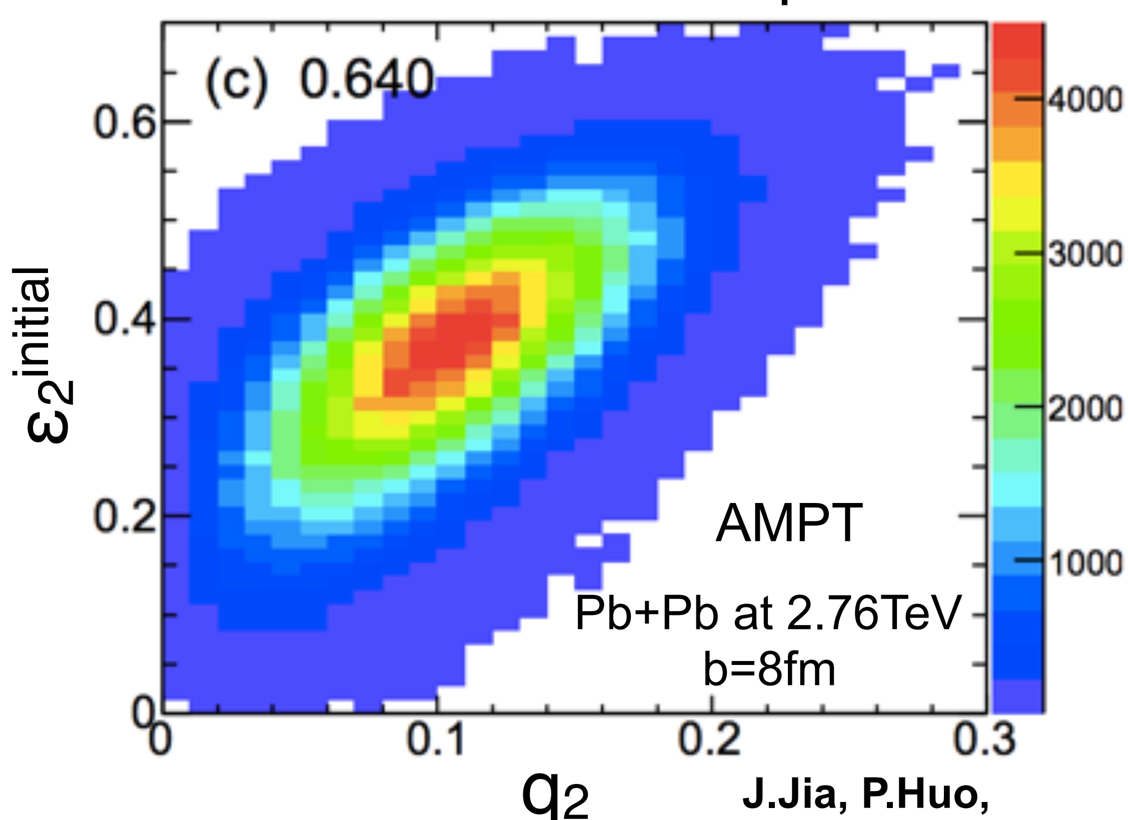

J.Jia, P.Huo, PRC 90 (2014), 034915

Separation of volume effect and geometry effect could be allowed

Motivation

- ✦ Combination of centrality selection and event shape engineering allows control of the initial geometry while keeping the average energy density (multiplicity) fixed
  - **Study difference of jet modification in medium expansion**
- ✦ Di-hadron correlations with event shape engineering allow new differential insight into energy loss mechanisms as a function of initial energy and shape
  - **Detailed information which was previously averaged out**

- ✦ **Analysis with minimum-bias Au+Au at $\sqrt{s_{NN}}$ = 200 GeV data collected by STAR in 2011**

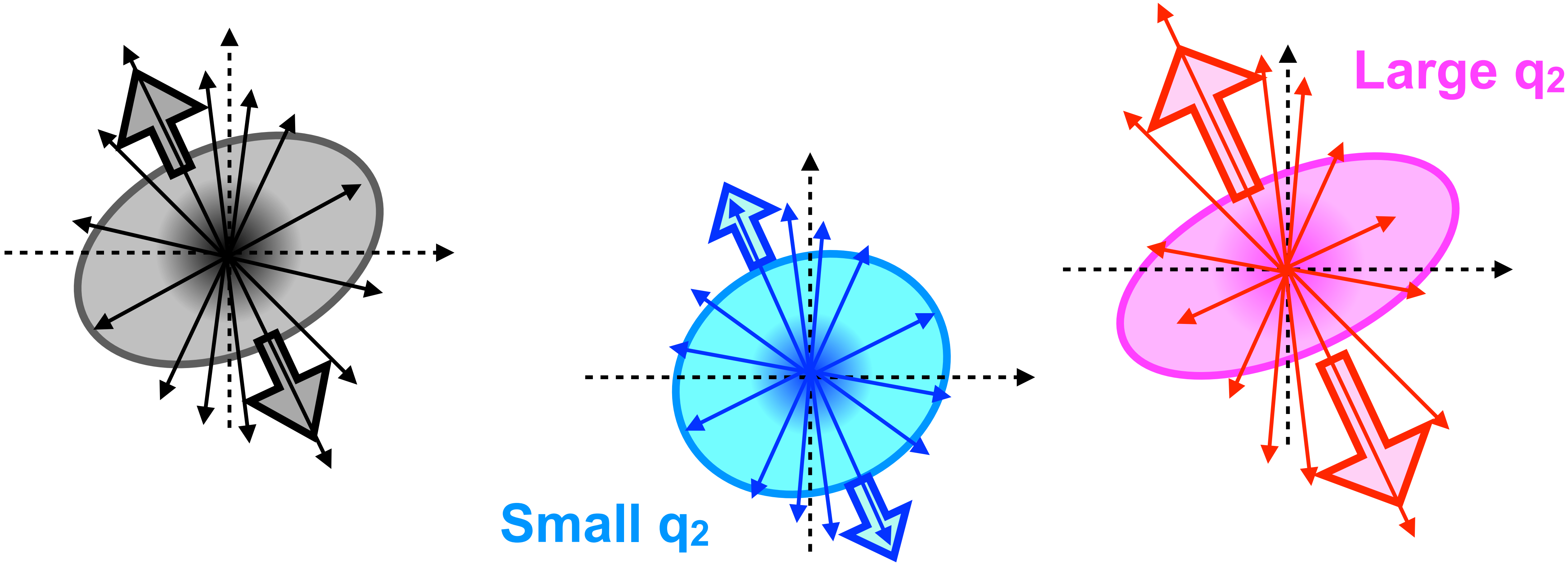

Data analysis

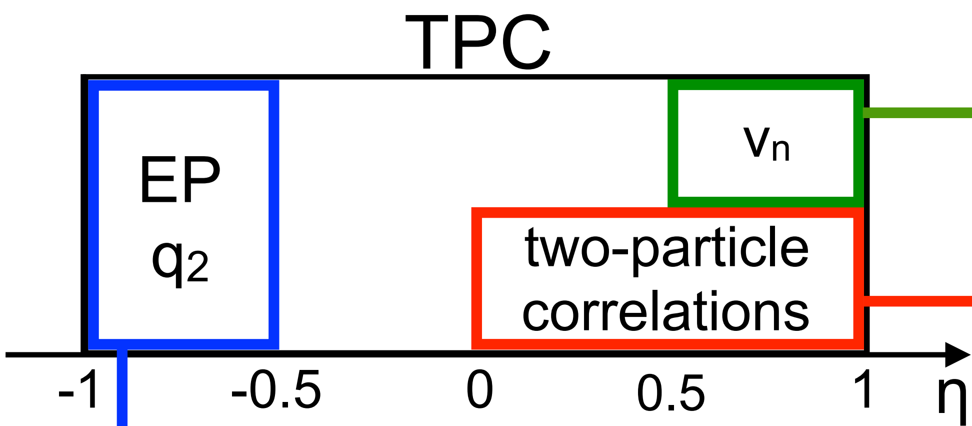

✦ **v_n measurement via EP method**

✦ **Two-particle correlations**

$$C(\Delta\phi) \propto \frac{N_{pair}^{real}(\Delta\phi)}{N_{pair}^{mix}(\Delta\phi)}$$

trigger angle selection w.r.t. EP

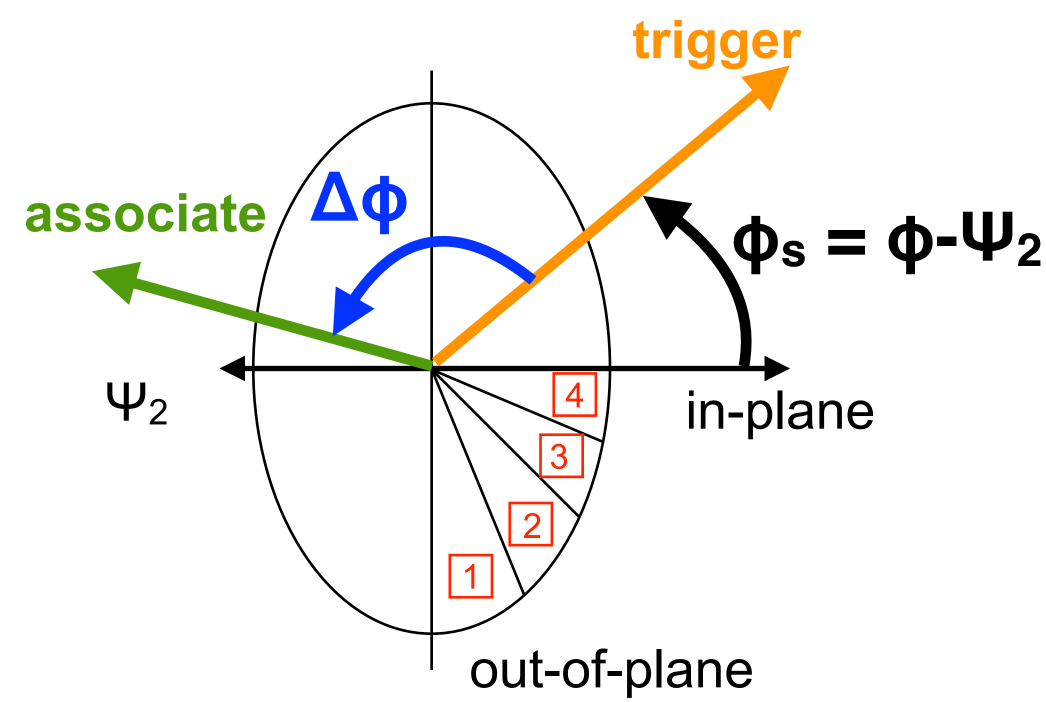

✦ **Event Plane Ψ_n**

✦ **q_2 selection**

- bottom 20% and top 20%

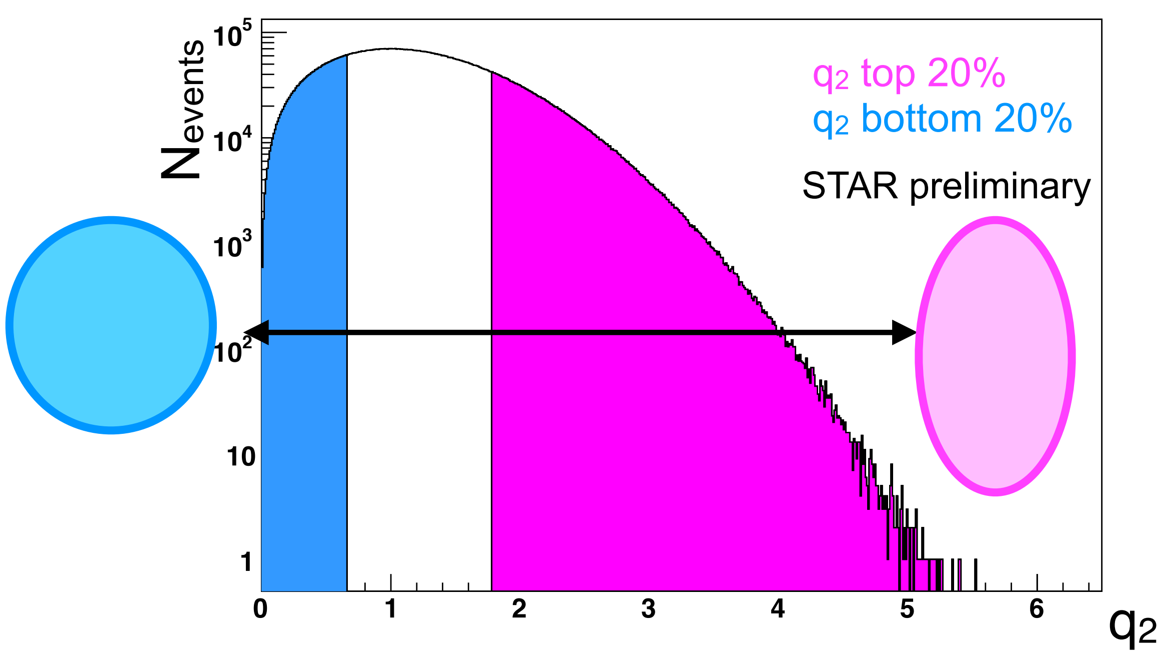

Background subtraction :

assuming ZYAM with inclusive-triggered correlations and subtract v_2, v_3 and v_4 contributions

Polar representation of correlated yield

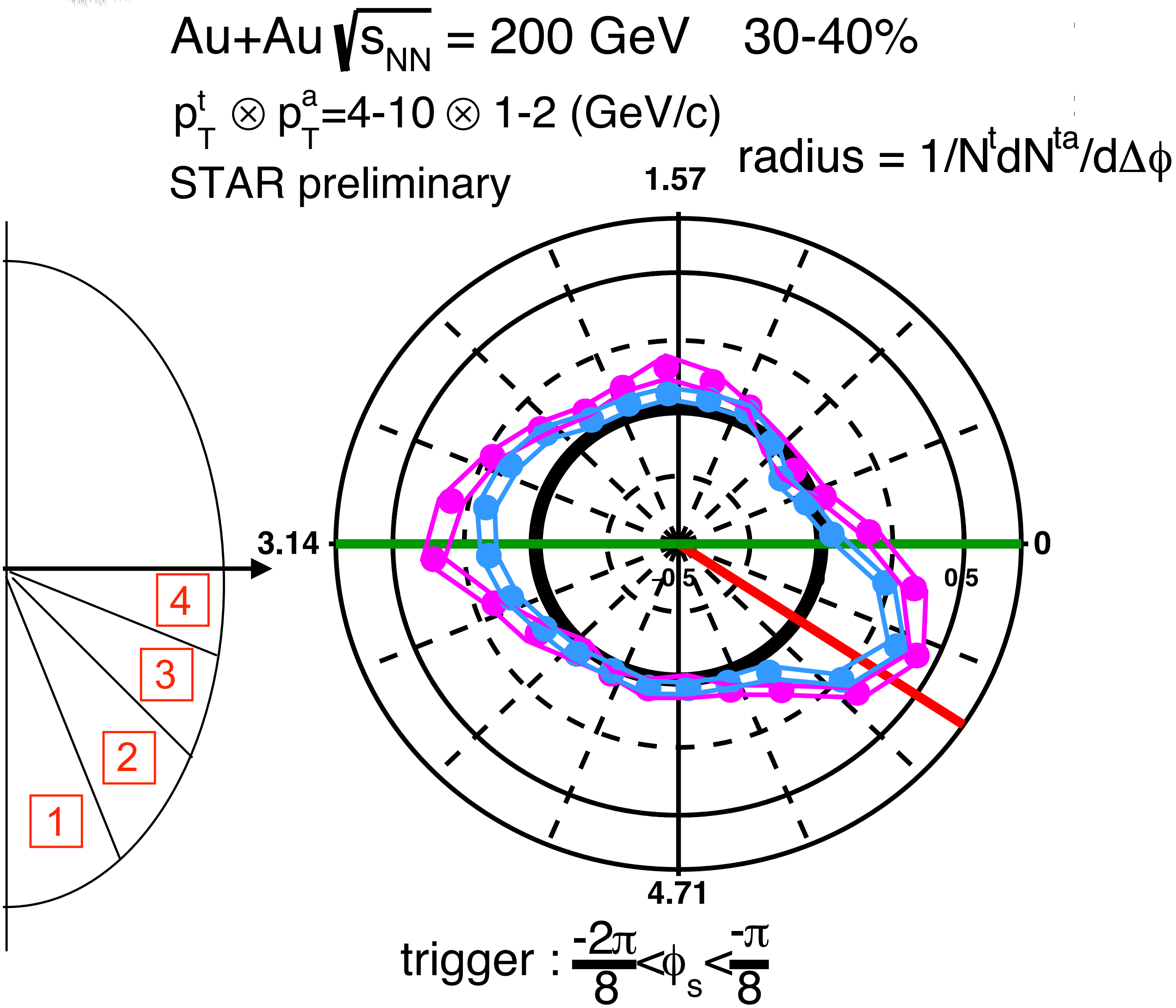

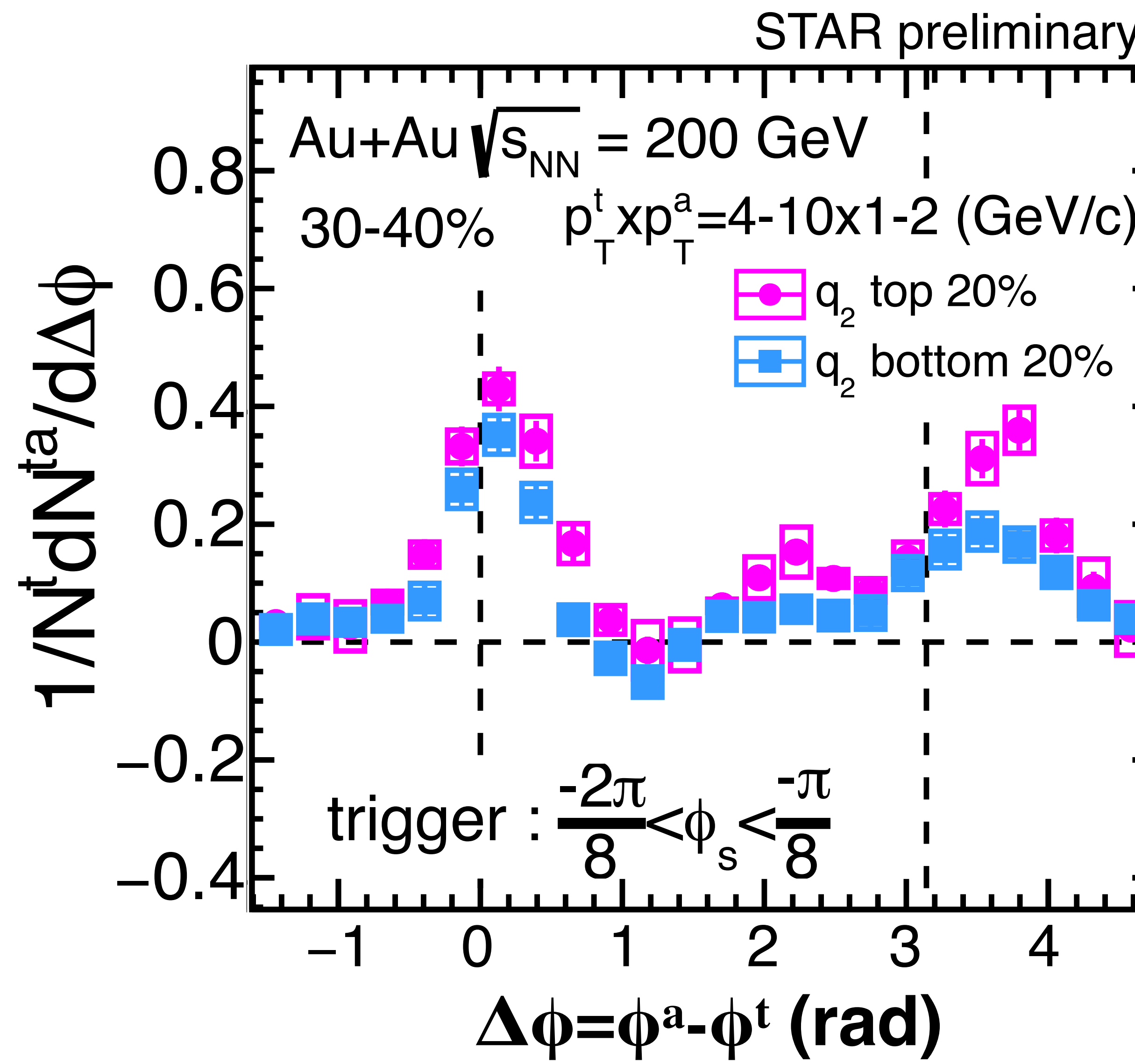

- ✦ Two axes should be considered : **back-to-back axis** and **EP axis**
  - ‣ Polar representations are displayed so that the correlation shapes are visually clear
- ✦ Relative angle Δϕ starts from red line and rotate toward counter-clockwise direction
- ✦ The amplitudes of correlated yield correspond to the radius

Polar representation of correlated yield

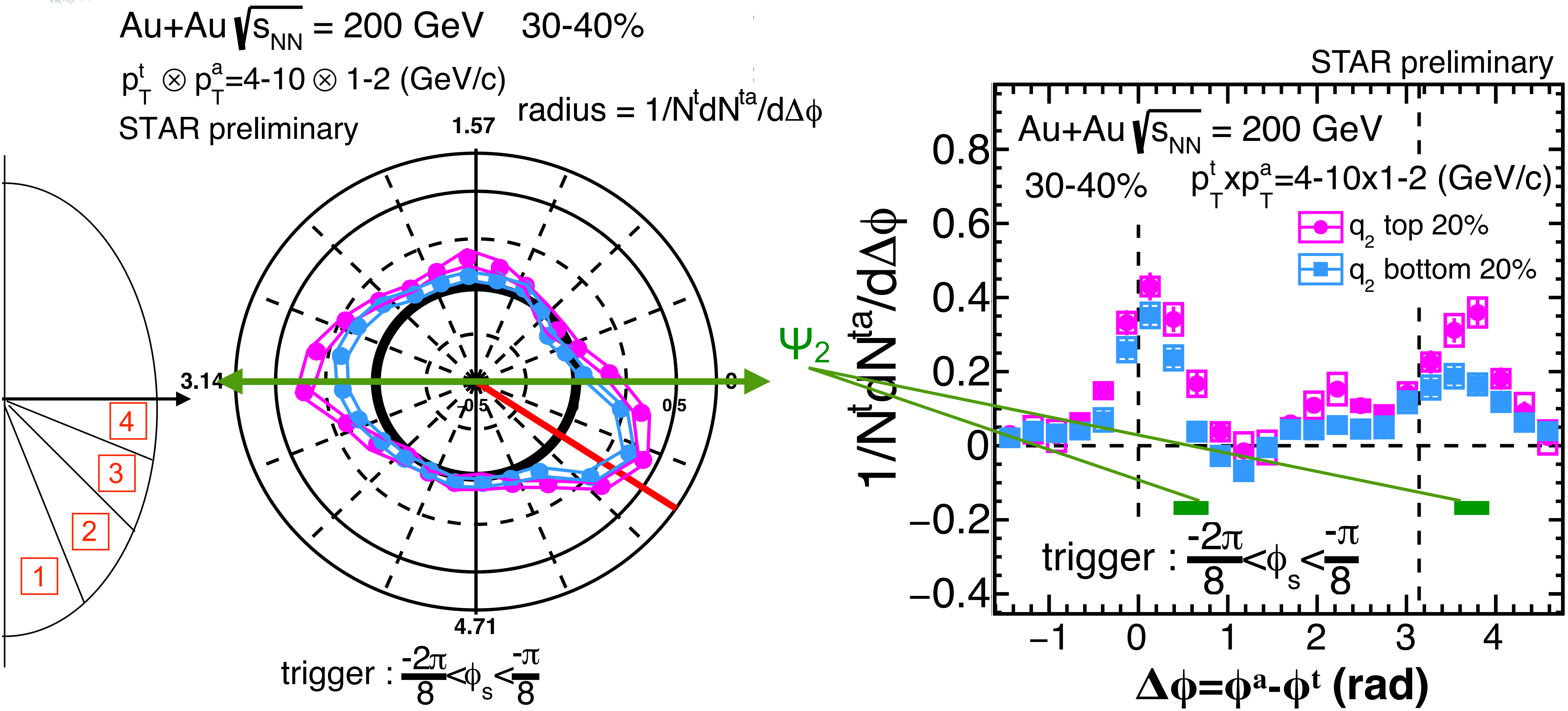

- ✦ Two axes should be considered : **back-to-back axis** and **EP axis**
  - Polar representations are displayed so that the correlation shapes are visually clear
- ✦ Relative angle $\Delta\phi$ starts from red line and rotate toward counter-clockwise direction
- ✦ The amplitudes of correlated yield correspond to the radius

Polar representation of correlated yield

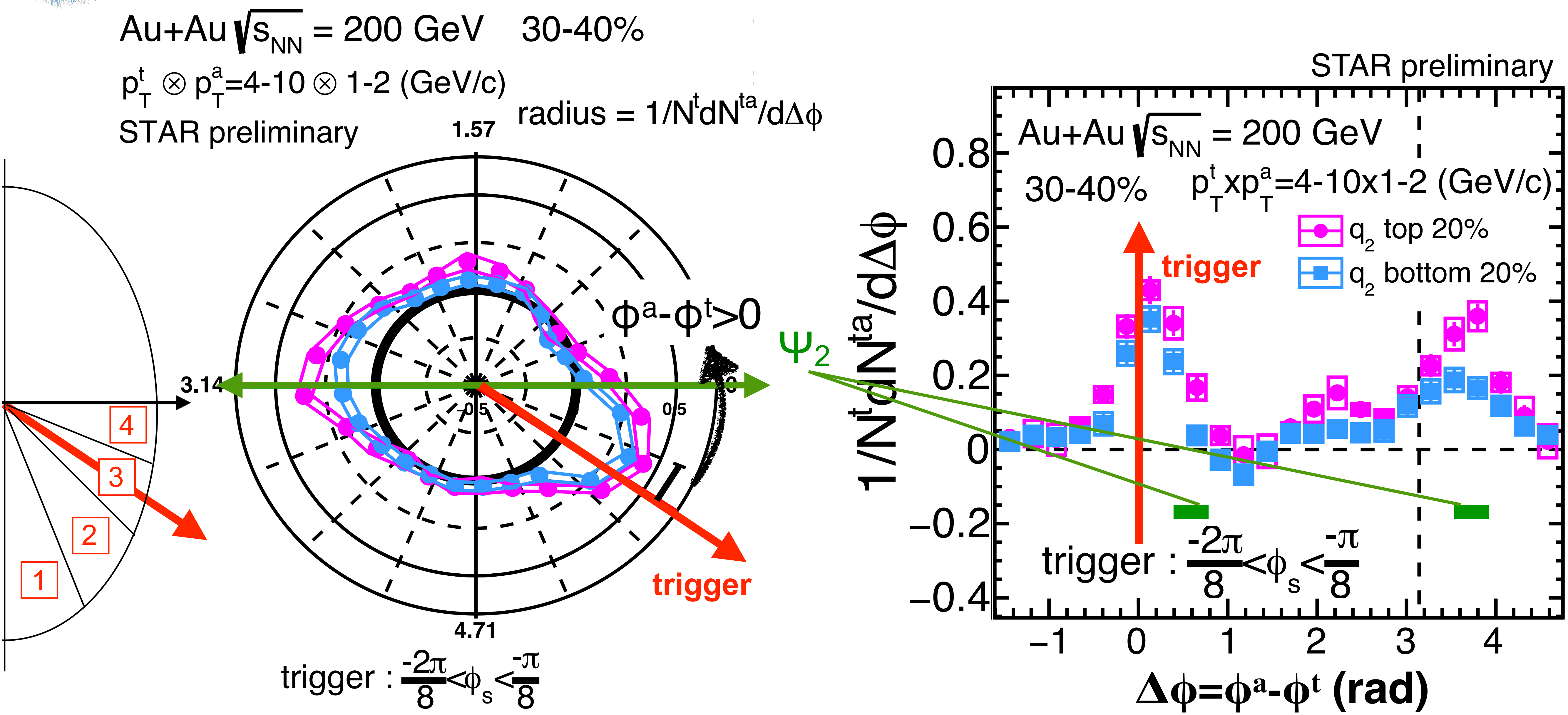

- ✦ Two axes should be considered : **back-to-back axis** and **EP axis**
  - Polar representations are displayed so that the correlation shapes are visually clear
- ✦ Relative angle $\Delta\phi$ starts from red line and rotate toward counter-clockwise direction
- ✦ The amplitudes of correlated yield correspond to the radius

Polar representation of correlated yield

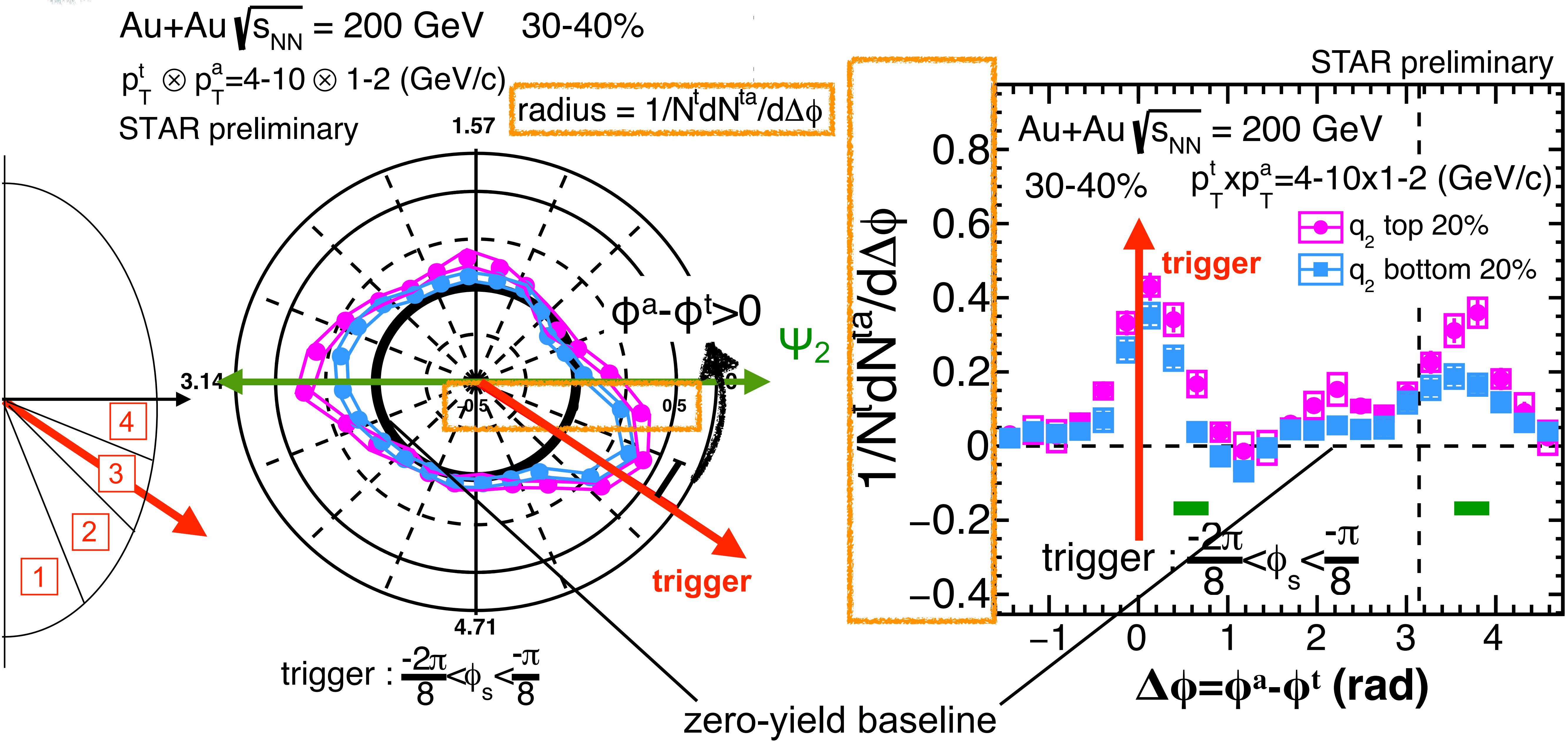

- Two axes should be considered : **back-to-back axis** and **EP axis**
  - Polar representations are displayed so that the correlation shapes are visually clear
- Relative angle $\Delta\phi$ starts from red line and rotate toward counter-clockwise direction
- The amplitudes of correlated yield correspond to the radius

Correlations after flow subtraction

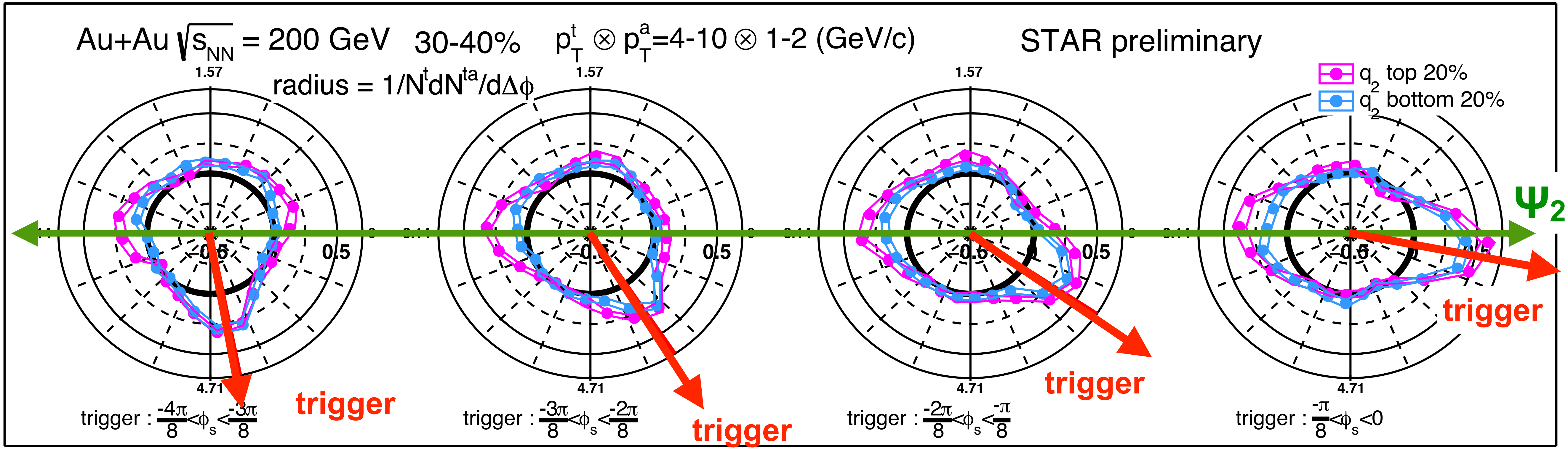

out-of-plane trigger ⟷ **in-plane trigger**

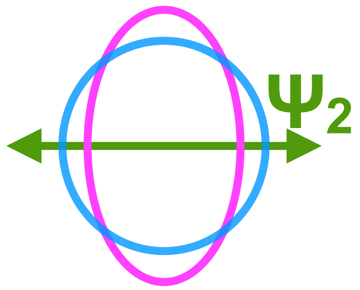

- **Near side**
  - No difference between large-q_2 and small-q_2 events with trigger out-of-plane
  - Peak height difference is enhanced with going to in-plane trigger
- **Away side**
  - Peaks are almost fully suppressed with trigger out-of-plane both in large-q_2 and small-q_2 events and remnant yield in the EP direction has q_2 dependence
  - Peak height difference is enhanced with going to in-plane trigger

➡ **Low-p_T particles preferentially escape toward in-plane direction?**

Summary

- ✦ **We measured di-hadron correlations with respect to the event plane with event shape engineering at the STAR experiment**
  - Separation between large-q_2 and small-q_2 events enhances difference of correlation shape while preserving average multiplicity
    ➡ new handle to differentially study partonic energy loss mechanisms

- ✦ Results for $4<p_T^{trig}<10$ GeV/c and $1<p_T^{asso}<2$ GeV/c in 30-40 % are shown in this talk
  - Centrality and p_T dependencies will be discussed in the future

Back up

v_2 with ESE

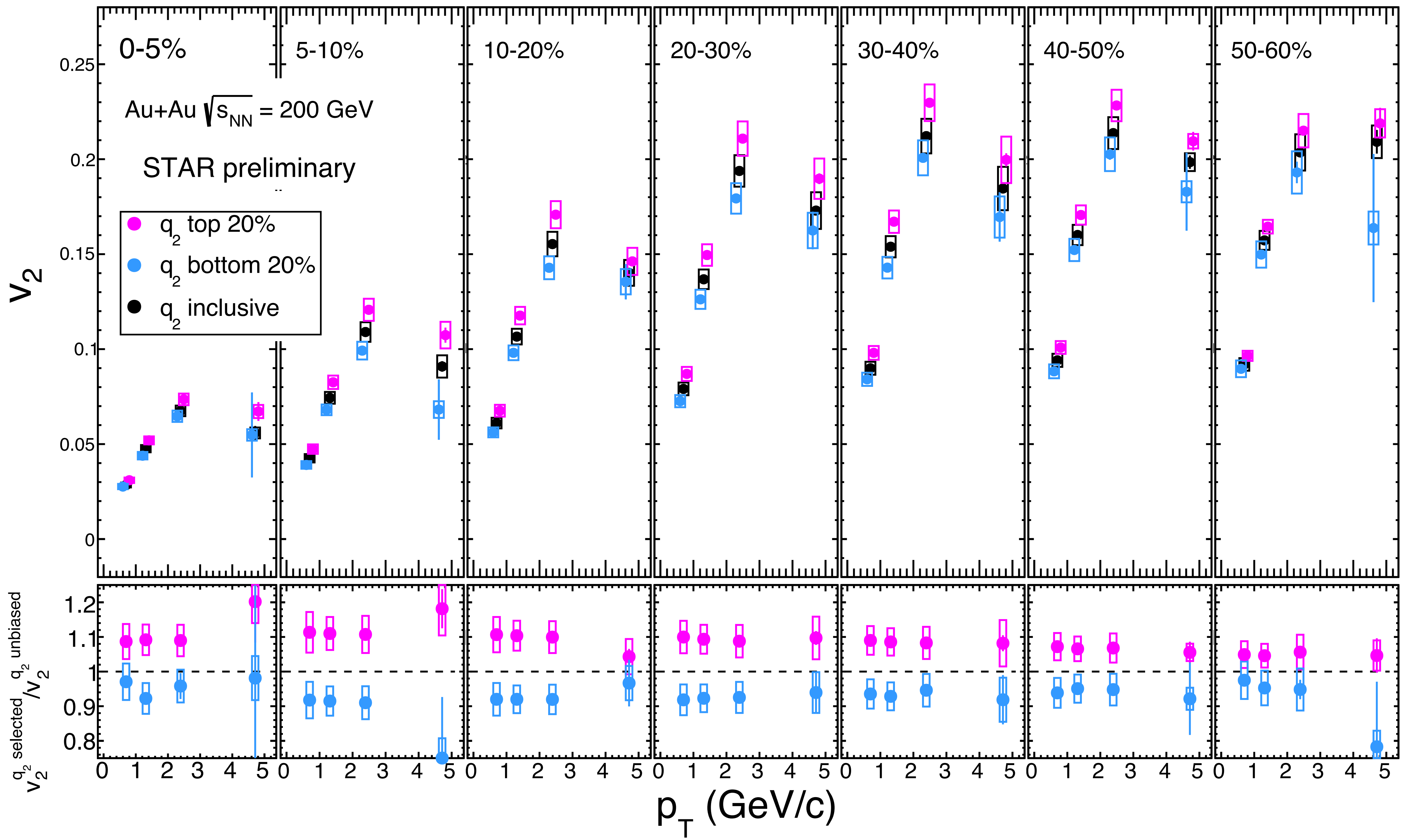

✦ v_2 is measured via event plane method with TPC-EP with taking 1.0 η gap

✦ 20% largest and smallest q_2 vectors are selected with the same region as TPC-EP

✦ Top 20% q_2 selection leads to **~10% larger v_2 events**

✦ Bottom 20% q_2 selection leads to **~8% smaller v_2 events**

Correlations with q_2 selection

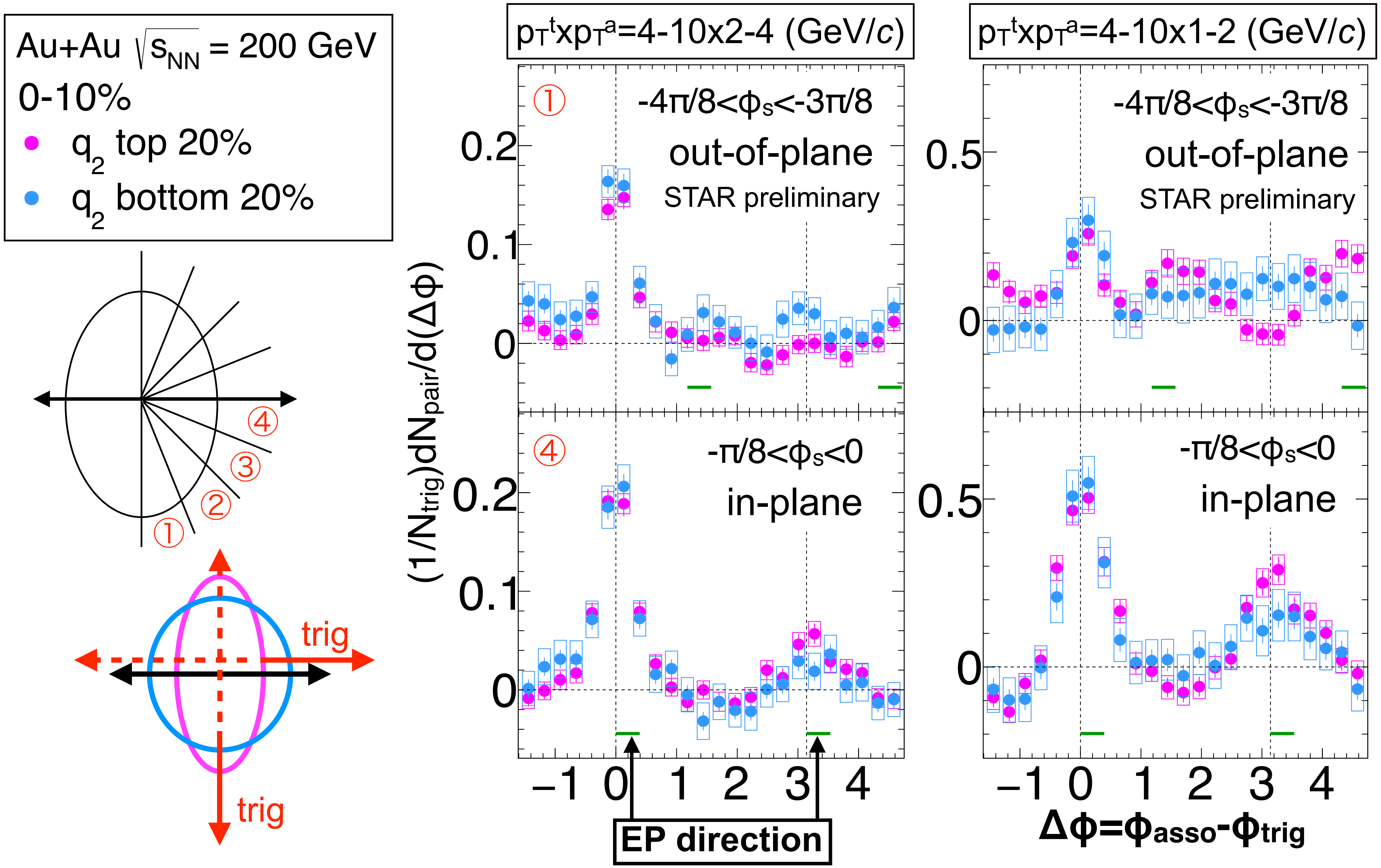

✦ High-p_T particles penetrate more with short path length

✦ Low-p_T particles are pushed toward in-plane direction and this effect is stronger in large q_2

➡ path-length dependent yield on the away side

Centrality dependence of mid-plane trigger

Au+Au $\sqrt{s_{NN}}$ = 200 GeV
$p_T^t \times p_T^a$=4-10x1-2 (GeV/*c*)
③ $-2\pi/8<\varphi_s<-\pi/8$

- q_2 top 20%
- q_2 bottom 20%

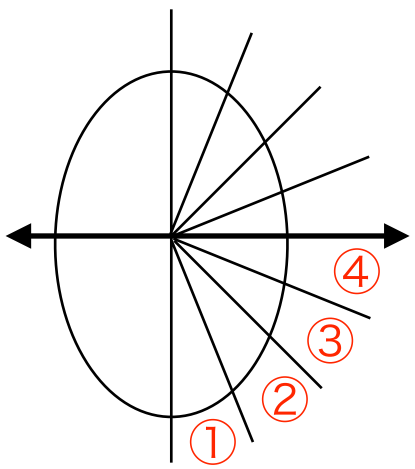

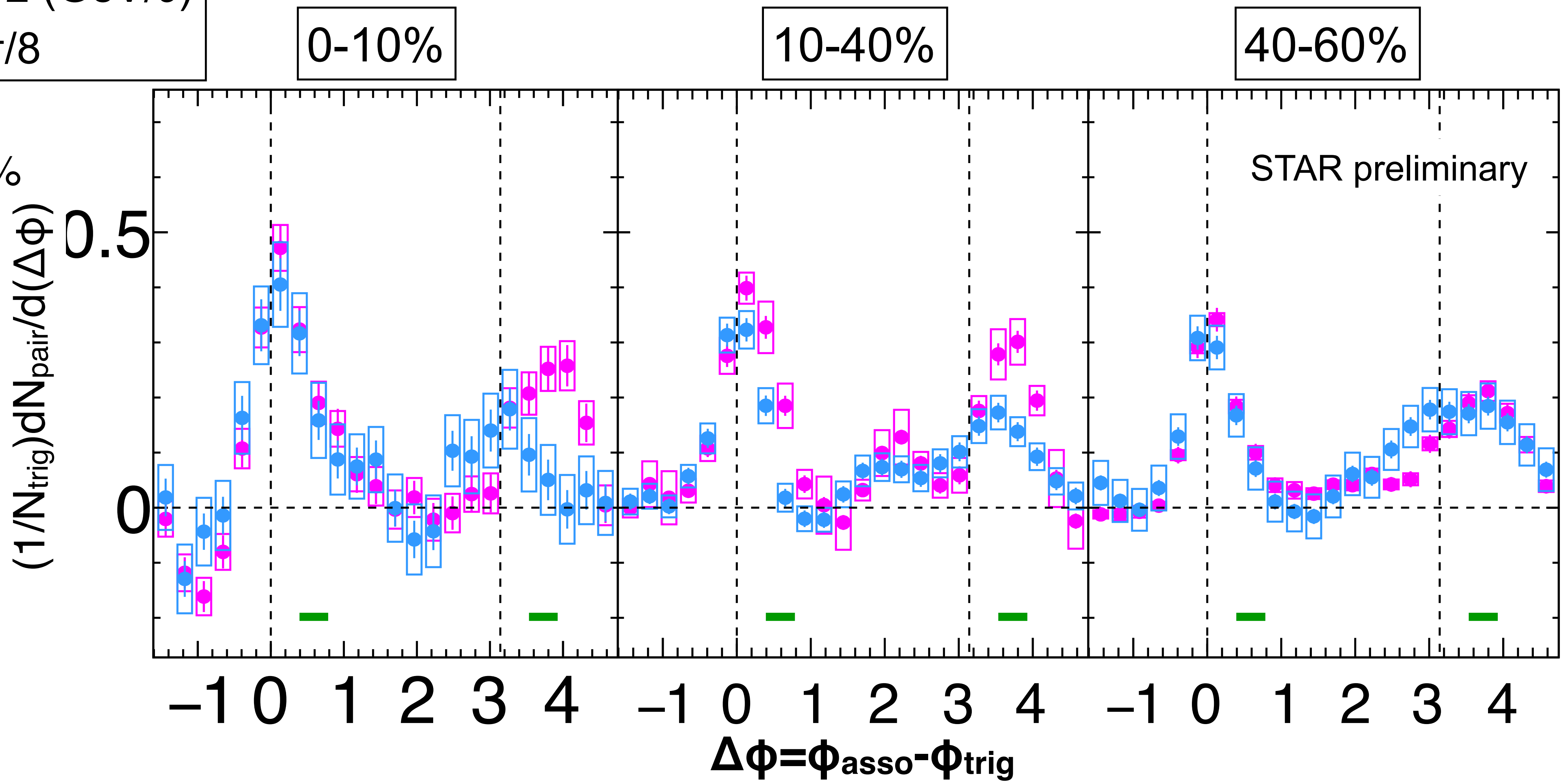

- ✦ See how shifting of away-side peak depends on centrality and q_2
- ✦ Large shift in large q_2 events
- ✦ q_2 dependence is stronger in central events
- ✦ No q_2 dependence in peripheral events

➡ Related to path-length or initial eccentricity?

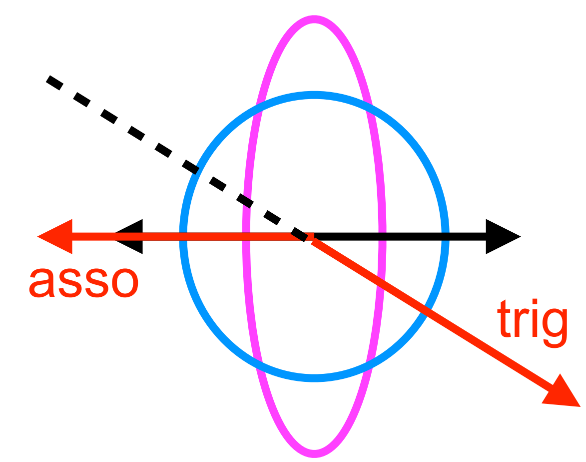

Comparison of polar and traditional distributions

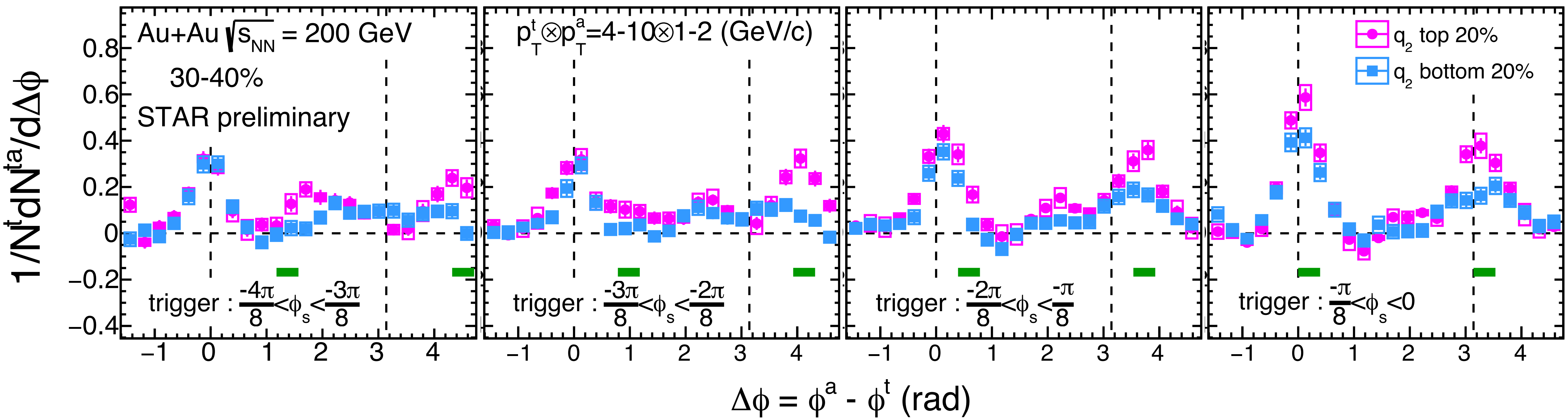

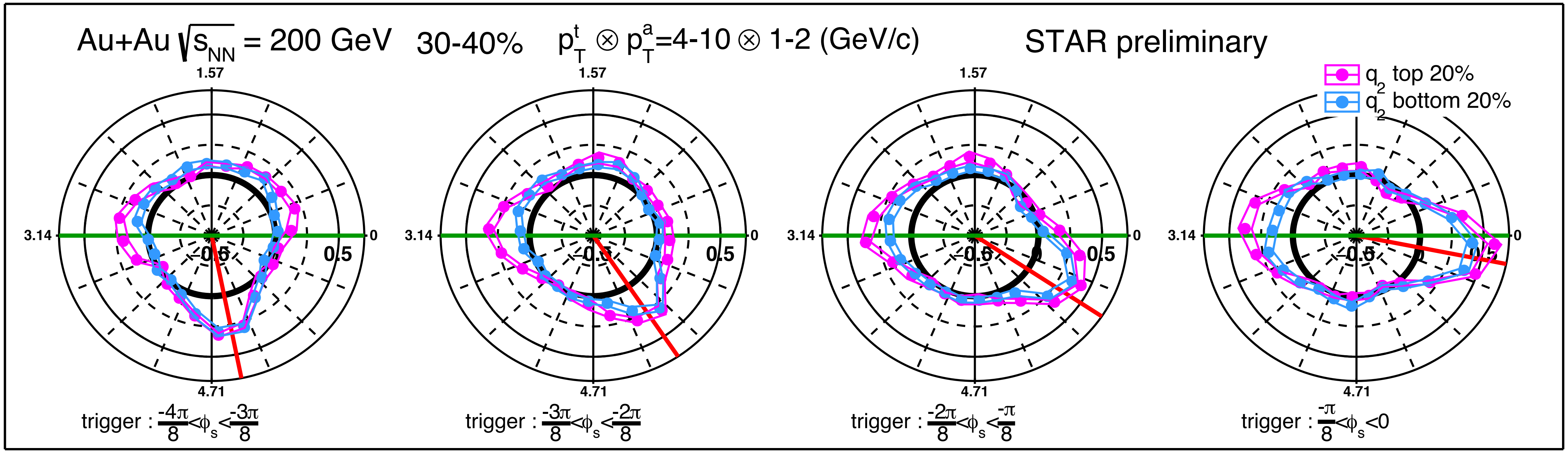

Resolution of EP

Au+Au $\sqrt{s_{NN}}$ = 200 GeV

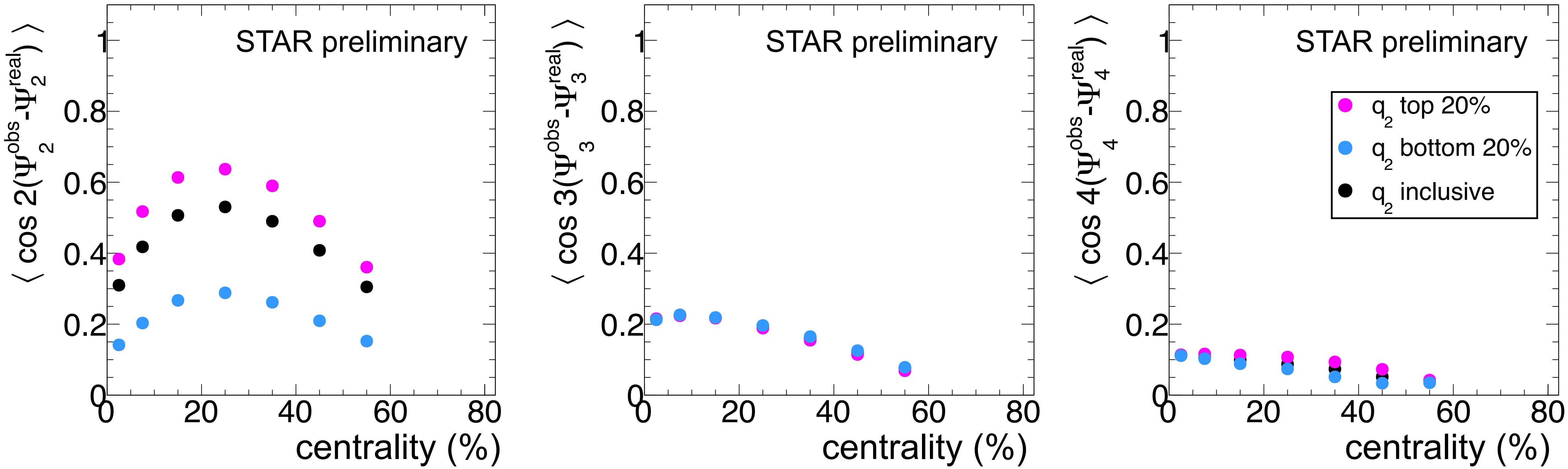

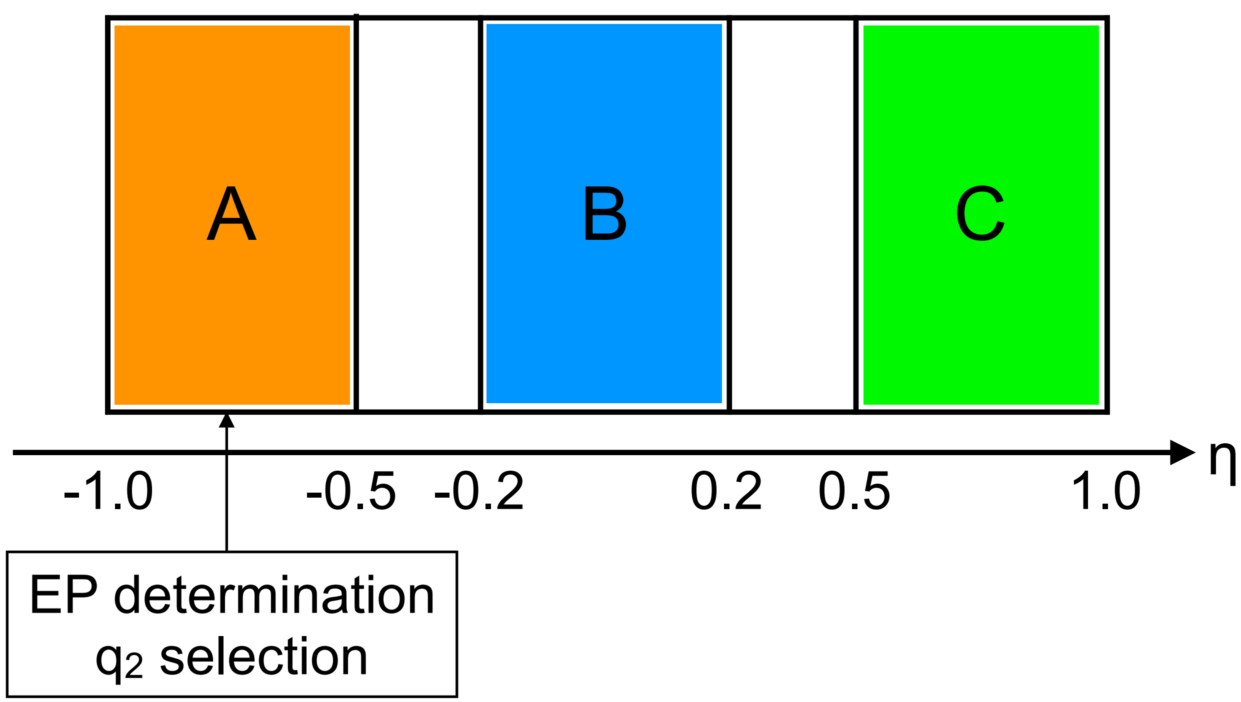

EP resolution via 3 sub-event method

$$\mathrm{Res}\{\Psi_n^A\} = \sqrt{\frac{\langle \cos n(\Psi_n^A - \Psi_n^B)\rangle \langle \cos n(\Psi_n^A - \Psi_n^C)\rangle}{\langle \cos n(\Psi_n^B - \Psi_n^C)\rangle}}$$

Res{Ψ_n^A} is shown in the upper figure

Data-driven flow MC simulation

Reconstruct flow distribution by Monte Carlo simulation

Input parameter : v_2, v_3, v_4, χ_{42}, and Res{Ψ_2}

1. generate Ψ_2, Ψ_3 at random and Ψ_4 with considering correlation between Ψ_2 and Ψ_4
2. make flow distribution which reproduce v_n
3. smear trigger particle's angle with probability distribution when selecting trigger particles angle
4. generate particles at random along the flow distribution and calculate $\Delta\phi$

Probability distribution can be written with χ_n which is calculated with following formula :

$$\langle \cos[kn(\Psi_n^{obs} - \Psi_n^{real})] \rangle = \frac{\sqrt{\pi}}{2\sqrt{2}} \chi_n e^{-\chi_n^2/4} \left[I_{(k-1)/2}\left(\frac{\chi_n^2}{4}\right) + I_{(k-1)/2}\left(\frac{\chi_n^2}{4}\right) \right]$$

Jean-Yves OLLITRAULT, PRD 48 (1993) 1132

example of probability distributions of $\Delta\Psi_2$

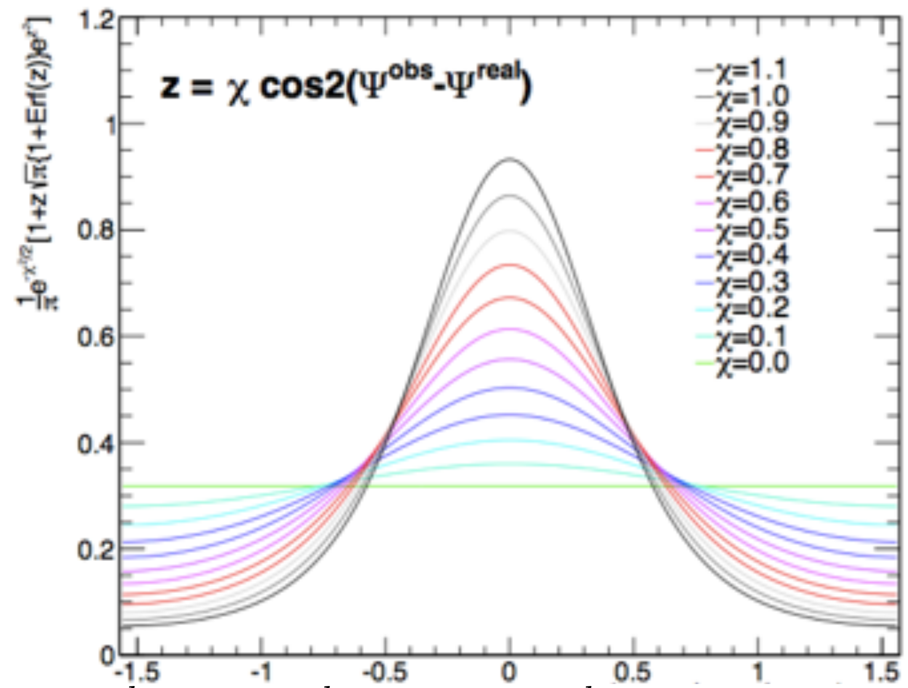

$$\Psi_n^{obs} - \Psi_n^{real} = (\phi^t - \Psi_n^{obs}) - (\phi^t - \Psi_n^{real})$$

Trigger smearing correction via fitting method

Assuming the associate-particles yield are distributed with respect to the event plane, we can correct the effect of trigger smearing due to the limited event-plane resolution which is similar to the resolution correction in the flow measurement of the single particles.

$$\frac{dN^{1+PTY}}{d(\phi^a-\Psi_2)} = 1+Y(\phi_s,\Delta\phi)$$
$$= 1+2v_2^Y\cos 2(\phi_s+\Delta\phi)+2v_4^Y\cos 4(\phi_s+\Delta\phi) \quad ...(1)$$

$$\phi_s+\Delta\phi = (\phi^t-\Psi_2)+(\phi^a-\phi^t) = \phi^a-\Psi_2$$

Applying a Fourier fitting eq.(3) to 1+Y(ϕ_s,$\Delta\phi$) as a function of ϕ_s with a phase shift $\Delta\phi$, v_n^Y can be determined and the azimuthal distributions can be corrected with corrected v_n^Y by the event-plane resolution eq.(5).

$$\frac{dN_{cor}^{1+PTY}}{d(\phi^a-\Psi_2)} = 1+2\frac{v_2^Y}{\sigma_2}\cos 2(\phi_s+\Delta\phi)+2\frac{v_4^Y}{\sigma_{42}}\cos 4(\phi_s+\Delta\phi) \quad ...(2)$$

$$F(\phi_s)^{raw} = 1+2v_2^{raw}\cos 2(\phi_s+\Delta\phi)+2v_4^{raw}\cos 4(\phi_s+\Delta\phi) \quad ...(3)$$
$$F(\phi_s)^{cor} = 1+2\frac{v_2^{raw}}{\sigma_2}\cos 2(\phi_s+\Delta\phi)+2\frac{v_4^{raw}}{\sigma_{42}}\cos 4(\phi_s+\Delta\phi) \quad ...(4)$$

$$1+Y^{cor}(\phi_s,\Delta\phi) = \frac{F(\phi_s)^{cor}}{F(\phi_s)^{raw}}\cdot(1+Y^{raw}(\phi_s,\Delta\phi)) \quad ...(5)$$

$\sigma_2 = \langle\cos 2(\Psi_2^{obs}-\Psi_2^{real})\rangle$
$\sigma_{42} = \langle\cos 4(\Psi_2^{obs}-\Psi_2^{real})\rangle$

PHENIX, PRC 84 (2011) 024904

Trigger smearing correction via iteration method

bin-by-bin iterative unfolding correction method for $Y(\Delta\varphi,\varphi_s)$

Y^{raw} : yield before correction
O : offset
$A^{(n)}$: n-th corrected data
$B^{(n)}$: n-th smeared correlation
$C^{(n)}$: n-th correction function
x,y : index of $\Delta\varphi$ and φ_s
Y^{corr} : yield after correction

input
(raw data) + offset

$A^{(0)} = Y^{raw}+O$

↓

smear (n-1)-th corrected data for φ_s direction with using probability distribution (P.21)

$B^{(n)} = SA^{(n-1)}$

→

make correction function ((n-1)-th corrected data) / (n-th smeared data)

$C^{(n)}(x,y) = A^{(n-1)}(x,y)/B^{(n)}(x,y)$

↓

smooth correction function with neighboring bins with using smoothing parameter

$C^{(n)}(x,y) = p_{\Delta\varphi}\{C^{(n)}(x-1,y)+C^{(n)}(x+1,y)\} + p_{\varphi s}\{C^{(n)}(x,y-1)+C^{(n)}(x,y+1)\}$

←

correction of raw data with n-th correction function

$A^{(n)}(x,y) = C^{(n)}(x,y)*A^{(0)}(x,y)$

↑ iteration (back to smearing step)

↓ after converge

output
(corrected data) - offset

$Y^{corr} = A^{(n)}-O$

Sources of systematics

- v_2, v_3 and v_4
  - including track cut, EP selection, and difference between v_n\{EP\} and v_n\{2PC\}
- EP resolution
  - difference between East and West for trigger smearing in toy-MC
- EP correlation between different order harmonics
  - only Ψ_2-Ψ_4 correlations
- $\Delta\phi$ range used for determination of zero-yield baseline
  - $\pi/6$ (default), $\pi/12$, $\pi/4$
- Trigger smearing correction
  - range of fitting method and iteration method
  - RMS of various smoothing parameter for ϕ_s and $\Delta\phi$